

Wettability of TiAl alloy melt on ceramic moulds in electromagnetic field

LI Bang-sheng(李邦盛)¹, LIU Ai-hui(刘爱辉)¹, NAN Hai(南海)²,
BI Wei-sheng(毕维生)¹, GUO Jing-jie(郭景杰)¹, FU Heng-zhi(傅恒志)¹

1. School of Materials Science and Engineering, Harbin Institute of Technology, Harbin 150001, China

2. Beijing Institute of Aeronautical Materials, Beijing 100095, China

Received 10 May 2007; accepted 29 November 2007

Abstract: In the electromagnetic field, the wettability between Ti50Al alloy melt and oxide ceramic moulds was studied by the self-designed measuring apparatus. The thermodynamic and kinetic laws and mechanism on wetting were studied systematically. The results show that in the electromagnetic field, the order of contact angles for the molten Ti50Al alloy for the eight oxide materials is $\theta(\text{Y}_2\text{O}_3) > \theta(\text{ZrO}_2(\text{Y}_2\text{O}_3)) > \theta(\text{ZrO}_2(\text{CaO})) > \theta(\text{CaO}) > \theta(\text{ZrO}_2(\text{MgO})) > \theta(\text{Al}_2\text{O}_3) > \theta(\text{Zircon}) > \theta(\text{MgO})$. The wetting process of Ti50Al alloy and ceramic moulds includes the nonreactive wetting at the first stage, and the reactive wetting at the final stage. And the higher the ceramic chemical stability, the longer the nonreactive wetting time.

Key words: TiAl alloy; ceramic; electromagnetic field; wettability; interfacial reaction

1 Introduction

For the high specific strength, excellent corrosion resistance and appropriate high temperature properties, TiAl alloys are potential high-temperature structural materials for aerospace and automobile applications [1–3]. Up to now, many researchers have developed TiAl components such as aviation engine blade, turbine disk, automobile engine blade wheel, and exhaust valve [4–8]. The above TiAl complex components can be processed by the investment casting technology, which is the optimal processing method for TiAl alloys. But the main problem of the investment casting is how to control the chemical reaction between high-activity TiAl alloys and molding materials [9–10].

In previous studies, the chemical reaction and the wettability at the interface were investigated as isolated subjects. However, they are closely linked with each other in reality. The wettability of TiAl alloy melt on ceramic materials is dependent on the interfacial reactivity. Thus it is necessary to improve the surface quality and mechanical properties by controlling the interfacial reaction between TiAl molten alloys and ceramic.

The sessile drop [11–12] is the most extensive

method used to measure the contact angle. But it is usually applied in the measurement of low-activity alloys, such as Al, Cu, Ni, Zn and Fe [13–15]. For high melting point and high reactivity of titanium alloys, the conventional sessile drop method is not suitable to measure the contact angle of molten titanium alloys/oxide ceramics, due to the fact that liquid metal reacts with ceramics, resulting in a new ceramic surface before titanium alloy melts into droplet. The contact angle measured after titanium alloy melting is not that between molten titanium alloys and initial ceramic substrates. Thus, the authors developed a testing device to measure the contact angle of high-activity metal melt on ceramics.

In the past decades, the electromagnetic, as a new physical field, has been widely used in advanced material processing. It is an attractive subject to study the precast-forming characteristics of titanium alloy components in the electromagnetic field. During the process of electromagnetic precast-forming, the contact angles between titanium alloy melt and ceramic moulds are very important for producing the high quality castings. However, so far, few researches have been done on the wettability between titanium alloys and ceramics in the electromagnetic field [16].

The major research work in the present work is that

by means of the contact angle testing device for the high-activity alloys, the wettability and reactivity between Ti50Al alloy melt and eight oxide ceramic substrates are investigated in the high-frequency electromagnetic field. And on the basis of thermodynamics, the wetting mechanism of molten Ti50Al alloy/ceramic system in the electromagnetic field is analyzed.

2 Experimental

The molding materials as substrates in this study were Y_2O_3 , MgO, Al_2O_3 , CaO, $ZrO_2(Y_2O_3)$ (namely, $ZrO_2(Y_2O_3)$ stabilized), $ZrO_2(CaO)$ (namely, $ZrO_2(CaO)$ stabilized), $ZrO_2(MgO)$ (namely, $ZrO_2(MgO)$ stabilized), and zircon, which were plates with 20 mm in diameter and 10 mm in thickness. The ceramic substrate was put on the graphite heating element, and then put into the induction coil of the testing device to measure the contact angle of high-activity metal melt on ceramics together. Fig.1 shows the apparatus for wetting experiments.

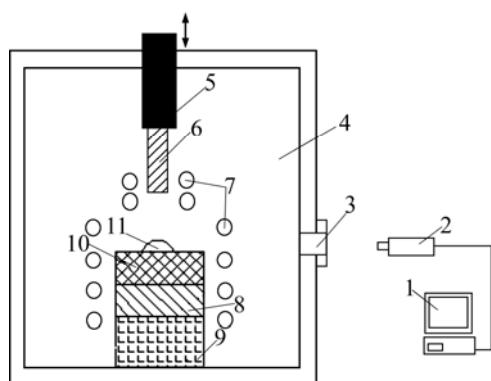


Fig.1 Schematic diagram of experimental apparatus: 1 Image processing system; 2 CCD video camera; 3 Quartz glass window; 4 Vacuum chamber; 5 Lift; 6 Ti50Al sample; 7 Induction coil; 8 Graphite; 9 Refractory; 10 Substrate; 11 Metal drop

Ti50Al alloy bar (5 mm in diameter) was employed in this study. It was ultrasound cleaned by acetone and ethanol and then dried in an air blast. Ti50Al alloy sample was held in the clamp of lift placed directly above the ceramic substrate. Before the heating cycle, the furnace chamber was evacuated down to 0.001 Pa and back-filled with argon gas two times, in order to reduce the oxygen content to a minimum level. After that, when the ceramic substrate was heated up to the Ti50Al alloy melting point by the graphite heating element, the end of Ti50Al alloy sample was put into the coil by lift. The high frequency induction coil in 50 kHz was used to heat Ti50Al alloy sample. As soon as the melting metal liquid dropped onto the ceramic substrates, the Ti50Al alloy sample was lift from the coil to avoid

the liquid metal dropping again. At the same time, the metal drop was held in the liquid state by the induction coil in 50 kHz, and images were obtained using a CCD camera and recorded on videotape at a speed of 6.3 frame/s. The contact angle was measured directly from the image of drop sections with an accuracy of $\pm 5^\circ$. All experiments were carried out with the same processing parameters.

3 Results and discussion

3.1 Wetting kinetics

The changes of contact angles with time are studied on Y_2O_3 , $ZrO_2(Y_2O_3)$, $ZrO_2(CaO)$, $ZrO_2(MgO)$, respectively. Fig.2 shows the video images of Ti50Al alloy droplets on the $ZrO_2(CaO)$ substrate at various time. Fig.3 presents the change curve of contact angle with time for the Ti50Al alloy and $ZrO_2(CaO)$. From Figs.2 and 3, it can be seen that the shape of the droplet is relatively smooth at the initial contact stage, and the angle changes little as time goes on. As the interfacial reaction of Ti50Al/ $ZrO_2(CaO)$ system takes place, the contact angle decreases. The system reaches the reactive wetting stage. The contact angle decreases obviously at 9 s and from 123° to 80° in 2 s. After this, the contact angle changes slowly. The chemical reaction is in equilibrium as the contact time is over 23 s, and the contact angle does not vary with time.

In contrast to the wetting dynamic process of Ti50Al/ $ZrO_2(CaO)$ stabilized), the non-reactive wetting of Ti50Al/ $ZrO_2(MgO)$ system is very fast (Fig.3), and the interfacial reaction takes place quickly in experiment. The contact angle decreases with the contact time from 1 s; the system transforms from the non-wetting to wetting and reaches equilibrium in 15 s. It is the MgO decomposition that accelerates the chemical reaction of system, reducing the time needed for the system to reach equilibrium.

In the electromagnetic field, in comparison with the changes of contact angles with time for the Ti50Al alloy and $ZrO_2(CaO)$, and $ZrO_2(MgO)$ systems as shown in Fig.3, it can be seen that for $ZrO_2(MgO)$ substrate the contact angle reduces rapidly from the first second, changes slowly after 5 s, and reaches constant after the following 15 s. On the contrary, the variation of contact angle with time for $ZrO_2(CaO)$ is not obvious during the first 9 s, indicating the Ti50Al/ $ZrO_2(CaO)$ system is at the non-reactive wetting stage. As the interfacial reaction between Ti50Al and $ZrO_2(CaO)$ takes place, the contact angle decreases greatly (after 9 s). The final contact angle is larger and the time reaching equilibrium is longer for Ti50Al/ $ZrO_2(CaO)$ than that for Ti50Al/ $ZrO_2(MgO)$.

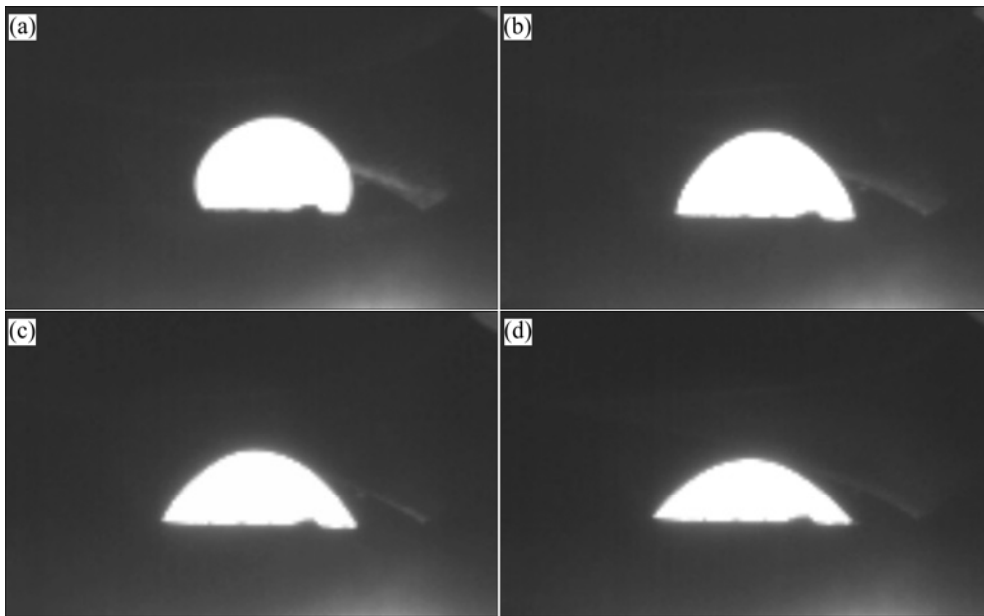


Fig.2 Images of Ti50Al droplets on $ZrO_2(CaO)$ substrates: (a) 1 s; (b) 10 s; (c) 20 s; (d) 30 s

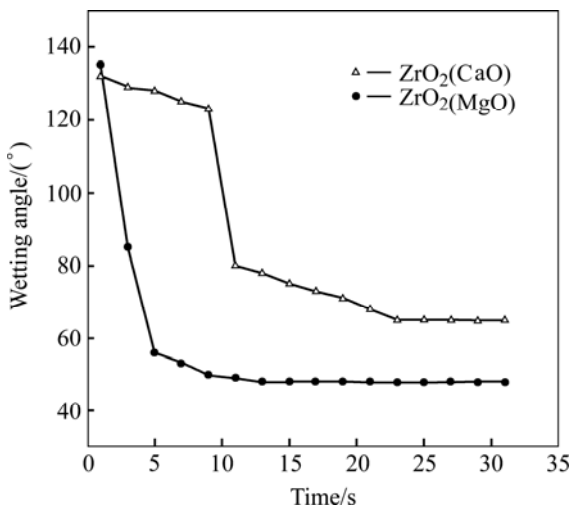


Fig.3 Curves of wetting angle vs time of Ti50Al/ $ZrO_2(CaO)$ and Ti50Al/ $ZrO_2(MgO)$

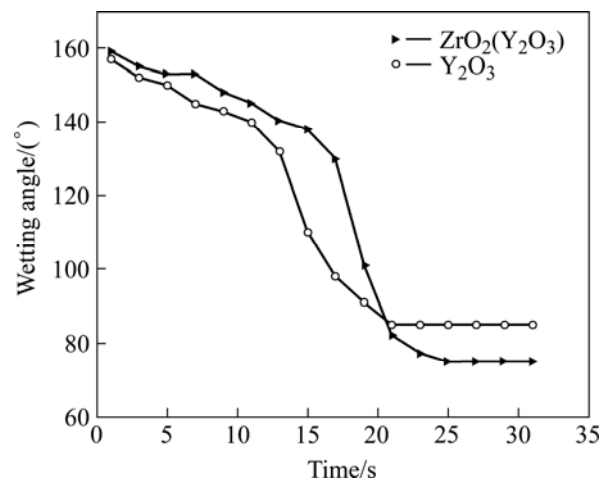


Fig.4 Curves of wetting angle vs time of Ti50Al/ $ZrO_2(Y_2O_3)$ and Ti50Al/ Y_2O_3

Fig.4 indicates the changes of contact angle with time for Y_2O_3 and $ZrO_2(Y_2O_3)$ substrates, respectively. It can be seen that the contact angles for Ti50Al/ Y_2O_3 and Ti50Al/ $ZrO_2(Y_2O_3)$ change gradually from the nonreactive wetting at the initial stage to the reactive wetting at the final stage, because Y_2O_3 and $ZrO_2(Y_2O_3)$, highly stable in the gravity field, react with molten Ti50Al alloy in the electromagnetic field. However, the changes of their contact angles are not obvious, because of highly stable Y_2O_3 governing the interfacial reaction speed and the spread of metal droplet on the ceramic substrates.

3.2 Wetting thermodynamics

The contact angles between molten Ti50Al alloys and eight ceramic materials are listed in Fig.5.

The order of the contact angles for the eight oxide molding materials is: $\theta(Y_2O_3) > \theta(ZrO_2(Y_2O_3)) > \theta(ZrO_2(CaO)) > \theta(CaO) > \theta(ZrO_2(MgO)) > \theta(Al_2O_3) > \theta(Zircon) > \theta(MgO)$. It is noted that Ti50Al alloy melt displays the best wettability against MgO, Al_2O_3 , and zircon, for contact angles less than 40° . The smallest contact angle of 25° is shown on the MgO ceramic substrate, and the biggest 85° on the Y_2O_3 . According to the thermodynamic stability of experimental molding materials at 1 770 K, SiO_2 in zircon is the lowest thermal stability. It reacts violently with Ti50Al alloy melt and forms more stable TiO so as to decrease the contact angle at high temperature. Although MgO is relatively thermodynamically stable compared with Al_2O_3 , it is still prone to decompose at high temperature due to its high vapor pressure. In vacuum, when MgO

contacts with Ti50Al alloy melt, it partially decomposes into element Mg and active O. The element Mg enters the furnace chamber in the form of gas, which provides a favorable condition for metal elements from Ti50Al alloy melt combining with active O. Meanwhile, the above combination in turn accelerates the decomposition process of MgO. Thus the contact angle of molten Ti50Al alloy on MgO is less than that on Al_2O_3 . For the Ti50Al/ Al_2O_3 system, the contact angle is also small because oxygen from Al_2O_3 combines with Ti from molten Ti50Al alloy to form fine TiO on the surface of Al_2O_{3-x} .

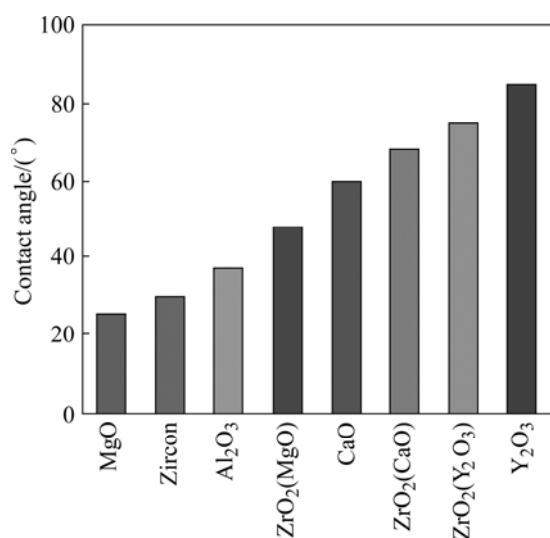


Fig.5 Contact angles between liquid Ti50Al and different moulds

The contact angle of Ti50Al alloy melt on $ZrO_2(MgO)$ is bigger than those on the three ceramic materials above, and smaller than those on Y_2O_3 , $ZrO_2(Y_2O_3)$, $ZrO_2(CaO)$. This is because the instability of Mg at high temperature enhances reactivity and intensifies the interfacial reaction so as to decrease the contact angle. Based on thermodynamic data, though CaO is more stable than ZrO_2 , the contact angle of Ti50Al alloy melt on CaO is smaller than that on $ZrO_2(CaO)$. It is because CaO reacting with Ti50Al alloy melt partially decomposes into element Ca and active O, and Ca is prone to enter the furnace chamber in the form of gas in vacuum. The thermodynamic stabilities of Y_2O_3 , $ZrO_2(Y_2O_3)$ and $ZrO_2(CaO)$ are the best with respect to molten Ti50Al alloys. Therefore, the contact angles of Ti50Al alloy melt on them are larger than on other ceramic materials, and the change of contact angles caused by interfacial reaction is not obvious.

3.3 Wetting mechanism of Ti50Al alloy melt/oxide ceramics in electromagnetic field

The dispersion force and Van der Waals force are

the main driving forces during wetting, when the liquid metal/solid ceramic interface is nonreactive. In this case, the wettability for the system is poor. The contact angle depends mainly on the surface energy of liquid metal/ceramic substrate, liquid metal/vapor, ceramic substrate/vapor, which can be expressed as the Yang equation for the conventional non-reactive wetting system:

$$\cos \theta = \frac{\sigma_{sl} - \sigma_{sg}}{\sigma_{lg}} \quad (1)$$

where θ is the contact angle; σ_{lg} , σ_{sg} and σ_{sl} are the surface tensions of liquid metal/vapor, ceramic/vapor and liquid metal/ceramic substrate, respectively.

However, besides physical action, there is chemical action between high-activity Ti50Al alloy melt and ceramic materials. On the basis of physical chemistry fundamentals, for the reactive system, the free energy change is induced because the nature of matter is changed through the chemical reaction, and the interaction between reactive product and liquid metal occurs. At a high temperature, highly chemical active Ti ions in molten Ti50Al alloy attract intensively O ion in ceramic materials. The greater the affinity of liquid metal and O, the greater the adhesive work, and the smaller the contact angle[17].

When liquid metal reacts with ceramic materials, which results in the formation of a continuous reactive product layer, the total free energy change at the liquid/solid interface, caused by interfacial reaction, is equal to the sum of free energy change produced by liquid metal reacting with ceramic materials and the interfacial energy of liquid metal/reactive product. LAURENT et al[18] introduced the chemical reaction free energy into Young equation and established the new contact angle formula in the reactive-wetting system:

$$\cos \theta' = \cos \theta - \Delta G_r / \sigma_{lg} - \Delta \sigma_r / \sigma_{lg} \quad (2)$$

where θ' is the contact angle of the high-activity liquid metal and ceramic mold after interfacial reaction, $\Delta \sigma_r$ is the interfacial energy change caused by interfacial composition change, ΔG_r is the Gibbs free energy change of interfacial reaction in the gravitational field.

According to Eqn.(2), though the interfacial reaction free energy change and the interfacial energy change caused by ceramic matrix composition are key factors affecting the system wettability, the interfacial reactive product is the covalent compound with stability close to ceramic matrix for the molten Ti50Al alloy/oxide ceramics system. Thus, at the interface the change of surface component of ceramic matrix is small, that is to say, the effect of $\Delta \sigma_r$ on the system wettability is weak, but the interfacial reaction free energy is large.

Consequently, the main driving force for improving the system wettability is the interfacial reaction free energy change of the molten Ti50Al alloy/oxide ceramic system.

It can also be found in Eqn.(2) that as ΔG_r increases, the θ' decreases and the wettability of liquid metal/ceramics is strengthened. In the electromagnetic field, due to the non-volume work done by electromagnetic field on the system, the free energy change caused by the chemical reaction in the electromagnetic field is greater than that in the gravity field, namely $|\Delta G_r| < |\Delta G_r'|$ ($\Delta G_r'$ is the free energy change for the liquid metal/ceramic system in the electromagnetic field). The contact angle for the liquid metal/ceramic system in the electromagnetic field is given as

$$\cos \theta'' = \cos \theta - \Delta G_r' / \sigma_{lg} - \Delta \sigma_r / \sigma_{lg} \quad (3)$$

where θ'' is the contact angle of the liquid metal/ceramic mold system in the electromagnetic field.

Comparing Eqns.(2) and (3), it is known that $\theta'' < \theta'$, that is to say, the contact angle of molten Ti50Al/oxide ceramics decreases.

4 Conclusions

1) The order of the contact angles of Ti50Al alloy melt on Y_2O_3 , $ZrO_2(Y_2O_3)$ stabilized), ZrO_2 (CaO stabilized), $ZrO_2(MgO)$ stabilized), CaO, MgO, Al_2O_3 and Zircon is $\theta(Y_2O_3) > \theta(ZrO_2(Y_2O_3)) > \theta(ZrO_2(CaO)) > \theta(CaO) > \theta(ZrO_2(MgO)) > \theta(Al_2O_3) > \theta(Zircon) > \theta(MgO)$. The contact angles between Ti50Al alloy and ceramic moulds increase with increasing the chemical stability of ceramic moulds.

2) The wetting process of Ti50Al alloy and ceramic moulds includes first stage of nonreactive wetting, and final stage of reactive wetting. And the higher the ceramic chemical stability, the longer the first stage time.

3) Based on the wetting experimental results between Ti50Al alloy melt and ceramic moulds, the wetting mechanism of molten Ti50Al alloy on the ceramic substrates is presented in the electromagnetic field. Compared with the gravity field, the contact angle for the reactive liquid metal/ceramic system is decreased extensively in the electromagnetic field. It is because the

non-volume work done by electromagnetic field on the system increases the free energy change caused by the chemical reaction in the gravity field.

References

- [1] BOYER R R. An overview on the use of titanium in aerospace industry [J]. *Materials Science and Engineering A*, 1996, 213: 103–114.
- [2] SCHUTZ R W, WATKINS H B. Recent developments in titanium alloy application in the energy industry [J]. *Materials Science and Engineering A*, 1998, 243: 305–315.
- [3] KIM Y W. Gamma titanium aluminides: Their status and future [J]. *JOM*, 1995, 7: 39–41.
- [4] LI Cheng-gong, FU Heng-zhi, YU Qiao. *Aeronautic and aerospace materials* [M]. Beijing: Defend Industry Press, 2001: 103–114. (in Chinese)
- [5] DIMIDUK D M. Gamma titanium aluminide alloys-an assessment within the competition of aerospace structural materials [J]. *Intermetallics*, 1998, 6: 709–713.
- [6] LORIA E A. Gamma titanium aluminides as prospective structural materials [J]. *Intermetallics*, 2000, 8: 1339–1345.
- [7] NODA T. Application of cast gamma TiAl for automobiles [J]. *Intermetallics*, 1998, 6: 709–713.
- [8] YAMAGUCHI M, INUI H, ITO K. High-temperature structural intermetallics [J]. *Acta Mater*, 2000, 48: 307–322.
- [9] SAHA R L, NANDY T K, MISRA R D K, JACOB K T. On the evaluation of stability of rare earth oxides as face coats for investment casting of titanium[J]. *Metallurgical Transactions B*, 1990, 21: 559–566.
- [10] LIN K F, LIN C C. Interfacial reactions between zirconia and titanium[J]. *Scripta Materialia*, 1998, 39(10): 1333–1338.
- [11] CONTRERAS A, LEON C A, DREW R A L, BEDOLLA E. Wettability and spreading kinetics of Al and Mg on TiC[J]. *Scripta Materialia*, 2003, 48: 1625–1630.
- [12] LAURENT V, CHATAIN D, EUSTATHOPOULOS. Wettability of SiC by aluminium and Al-Si alloys[J]. *Journal of Materials Science*, 1987, 22: 244–250.
- [13] ZHOU X B, HOSSON J T D. Reactive wetting of liquid metals on ceramics substrates [J]. *Acta Mater*, 1996, 44(2): 421–426.
- [14] SHINOZAKI N, SONODA M, MUKAI K. Wettability, surface, tension, and reactivity of the molten manganese/zirconia-yttria ceramic system[J]. *Metallurgical and Materials Transactions A*, 1998, 29: 1121–1125.
- [15] SHEN P, HIDETOSHI F, TAIHEI M, KIYOSHI N. Reactive wetting of SiO_2 substrates by molten Al[J]. *Metallurgical and Materials Transactions A*, 2004, 35: 583–588.
- [16] ZHU Jun, KAMIYA A. Surface tension, wettability and reactivity of molten titanium in Ti/yttria-stabilized zirconia system [J]. *Materials Science and Engineering A*, 2002, 237: 117–127.
- [17] UEKI M, NAKA M, OKAMOTO I. Wettability of some metals against zirconia ceramics[J]. *Journal of Materials Science Letters*, 1986, 5(12): 1261–1262.
- [18] LAURENT V, CHATAIN D, EUSTATHOPOULOS. Wettability of SiO_2 and oxidized SiC by aluminium [J]. *Materials Science and Engineering A*, 1991, 135: 89–94.

(Edited by YUAN Sai-qian)